

## Diboson Production at the Tevatron

Ia Iashvili

SUNY, Buffalo, NY 14260, USA

We present the latest results on the production of  $WW$ ,  $WZ$ ,  $W\gamma$ ,  $Z\gamma$  and  $ZZ$  events at the Fermilab Tevatron Collider. The results are based on the analyses of  $0.2 - 2 \text{ fb}^{-1}$  of data collected in  $p\bar{p}$  collisions at  $\sqrt{s} = 1.96 \text{ TeV}$  by CDF and  $D\bar{O}$  experiments during the Tevatron Run II. Analyses of the diboson production processes provide crucial test of the Standard Model, directly probing its predictions on the Trilinear Gauge Couplings.

## I. INTRODUCTION

The Standard Model (SM) makes precise predictions for the couplings between gauge bosons thanks to the non-abelian nature of its  $SU(2)_L \times U(1)_Y$  symmetry. These self-interactions are described by the trilinear  $WW\gamma$ ,  $WWZ$ ,  $Z\gamma\gamma$  and  $ZZ\gamma$  and  $ZZZ$  gauge couplings (TGCs), which can be directly tested in the pair productions of the gauge bosons. Therefore datasets of  $WW$ ,  $W\gamma$ ,  $Z\gamma$ ,  $WZ$  and  $ZZ$  candidate events produced in  $p\bar{p}$  collisions at  $\sqrt{s} = 1.96 \text{ TeV}$  at the Tevatron  $p\bar{p}$  Collider provide crucial testing ground for SM. Any deviations from the SM predictions can indicate presence of New Physics. Furthermore, diboson processes have signatures similar to that of the Higgs production at the Tevatron, and constitute background to the Higgs searches. Thus detailed understanding of the diboson processes at the Tevatron is viewed as a first step towards probing the Higgs boson production.

Production cross sections for the diboson processes at the Tevatron are a few orders of magnitude smaller compared to that of the inclusive  $W$  and  $Z$  productions. Diboson events with the leptonic decays of  $W$  and  $Z$  bosons provide final states with the lowest background contamination, but also suffer from small branching ratios.

The Tevatron Collider has already delivered more than  $4 \text{ fb}^{-1}$  of data to the CDF and  $D\bar{O}$  experiments. These large datasets allow to probe the diboson processes even with very small production cross section times branching fraction, of the order of a few femtobarns. The results presented here are based on  $0.2 - 2 \text{ fb}^{-1}$  of data.

II.  $WW \rightarrow \ell\nu\nu$  PRODUCTION

Pair production of the  $W$  bosons at the Tevatron,  $p\bar{p} \rightarrow W^+W^-$ , proceeds through  $Z/\gamma$  exchange. Thus  $WW$  events allow to probe trilinear  $WWZ/WW\gamma$  couplings. Furthermore,  $W^+W^-$  events are dominant irreducible background to the Higgs searches in the  $H \rightarrow W^+W^-$  channel, and their understanding is important. When followed by leptonic decays,  $W \rightarrow \ell\nu$  ( $\ell = e$  or  $\mu$ ), of both  $W$ s,  $WW$  production leads to final states with two high- $p_T$  isolated leptons of opposite sign,  $e^\pm e^\mp$ ,  $\mu^\pm \mu^\mp$  or  $e^\pm \mu^\mp$ , and large transverse missing energy,  $E_T^{miss}$ , due to escaping neutrinos. There are many other SM processes which can give the similar event signature:  $W(\rightarrow \ell\nu) + \text{jets}$  production with a jet faking electron or containing muon,  $Z/\gamma^* \rightarrow \ell\ell$ ,  $t\bar{t}$ ,  $WZ$  and  $ZZ$  processes can all contribute to the background. Signal separation from the background is achieved by rejecting  $e^+e^-$  and  $\mu^+\mu^-$  events with dilepton mass consistent to  $M_Z$ , by vetoing large hadronic activities, and removing events where missing  $E_T$  is likely to have originated from jet mis-measurements. The  $WW$  production signal has been established by both,  $D\bar{O}$  and CDF Collaborations with already  $\simeq 240 \text{ pb}^{-1}$  [1] and  $\simeq 200 \text{ pb}^{-1}$  [2] of data, respectively. The measured cross sections of  $\sigma(WW) = 13.8_{-3.8}^{+4.3}$  (stat)  $_{-0.9}^{+1.2}$  (syst)  $\pm 0.9$  (lumi) pb [1] by  $D\bar{O}$ , and  $\sigma(WW) = 13.6 \pm 2.3$  (stat)  $\pm 1.6$  (syst)  $\pm 1.2$  (lumi) pb by CDF using  $\mathcal{L} \simeq 825 \text{ pb}^{-1}$  of data [3], are in

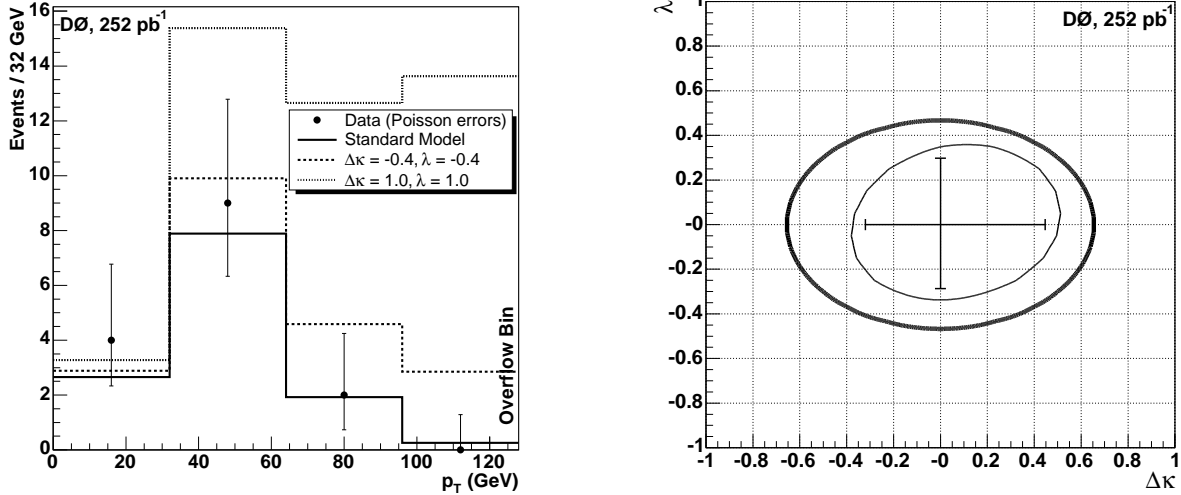


FIG. 1: Left: Distribution of the leading lepton  $p_T$  for  $WW \rightarrow e^\pm \mu^\mp$  candidates in  $D\bar{0}$  data, and expectations from the SM (solid line) and two anomalous coupling scenarios (dashed lines) [8]. Right: One- (ticks along the axes) and two-dimensional (the inner curve) 95% C.L. limits at  $\Lambda = 2.0$  TeV assuming equal  $WWZ$  and  $WW\gamma$  couplings. The bold curve is the unitarity limit. The limits are obtained from  $D\bar{0} WW \rightarrow \ell^\pm \ell^\mp$  analysis [8].

agreement with a SM Next-to-Leading Order (NLO) prediction of 12.0 – 13.5 pb [4, 5].

The general Lorentz invariant effective Lagrangian describing  $WWV$  ( $V = \gamma$  or  $Z$ ) vertices [6, 7] has seven parameters for each of the  $WW\gamma$  and  $WWZ$  vertices. With the assumption of electromagnetic gauge invariance and C and P conservation, the number of independent couplings is reduced to five, and the Lagrangian takes the form:

$$\frac{\mathcal{L}_{WWV}}{g_{WWV}} = ig_1^V (W_{\mu\nu}^\dagger W^\mu V^\nu - W_\mu^\dagger V_\nu W^{\mu\nu}) + i\kappa_V W_\mu^\dagger W_\nu V^{\mu\nu} + \frac{i\lambda_V}{M_W^2} W_\lambda^\dagger W_\mu^\nu V^{\nu\lambda} \quad (1)$$

where  $W^\mu$  is the  $W^-$  field,  $W_{\mu\nu} = \delta_\mu W_\nu - \delta_\nu W_\mu$ ,  $V_{\mu\nu} = \delta_\mu V_\nu - \delta_\nu V_\mu$ , and  $g_1^\gamma = 1$ . The overall couplings are  $g_{WW\gamma} = -e$  and  $g_{WWZ} = -e \cot\theta_W$ . The five remaining parameters are  $g_1^Z$ ,  $\kappa_Z$ ,  $\kappa_\gamma$ ,  $\lambda_Z$ , and  $\lambda_\gamma$ . In the SM,  $g_1^Z = \kappa_Z = \kappa_\gamma = 1$  and  $\lambda_Z = \lambda_\gamma = 0$ . The couplings  $g_1^Z$ ,  $\kappa_Z(\gamma)$  are often written in terms of their deviation from the SM values as  $\Delta g_1^Z = g_1^Z - 1$ ,  $\Delta\kappa_{Z(\gamma)} = \kappa_{Z(\gamma)} - 1$ .

One effect of introducing anomalous coupling parameters into the SM Lagrangian is an increase of the cross section for the  $q\bar{q} \rightarrow Z/\gamma \rightarrow W^+W^-$  production with increasing parton center-of-mass energy  $\sqrt{\hat{s}}$ . To keep the cross section from diverging, the anomalous coupling must vanish as  $s \rightarrow \infty$ . This is achieved by introducing a dipole form factor for arbitrary coupling  $\alpha$  ( $g_1^Z$ ,  $\kappa_Z$ ,  $\kappa_\gamma$ ,  $\lambda_Z$  or  $\lambda_\gamma$ ):  $\alpha(\hat{s}) = \frac{\alpha_0}{(1 + \frac{\hat{s}}{\Lambda^2})^2}$ , where the form factor  $\Lambda$  is set by new physics. For a given value of  $\Lambda$ , there is an upper limit on the size of the coupling, beyond which unitarity is exceeded.

TABLE I: One-dimensional 95 % C.L. limits with various assumptions relating the  $WW\gamma$  and  $WWZ$  couplings and various values of form factor scale  $\Lambda$ . Parameters that are not constrained by the coupling relationships are set to their SM values. The limits are obtained in  $D\bar{0} WW$  analysis [8]

Assumptions on couplings and $\Lambda$	$WW\gamma = WWZ$ $\Lambda = 1.5$ TeV	$WW\gamma = WWZ$ $\Lambda = 2.0$ TeV	$HISZ$ $\Lambda = 1.5$ TeV	$SMWW\gamma$ $\Lambda = 2.0$ TeV	SM $WWZ$ $\Lambda = 1.0$ TeV
95% C.L.	$-0.31 < \lambda < 0.33$	$-0.29 < \lambda < 0.30$	$-0.34 < \lambda < 0.35$	$-0.39 < \lambda_Z < 0.39$	$-0.97 < \lambda_\gamma < 1.04$
Limits	$-0.36 < \Delta\kappa < 0.47$	$-0.32 < \Delta\kappa < 0.45$	$-0.57 < \Delta\kappa_\gamma < 0.75$	$-0.45 < \Delta\kappa_Z < 0.55$	$-1.05 < \Delta\kappa_\gamma < 1.29$

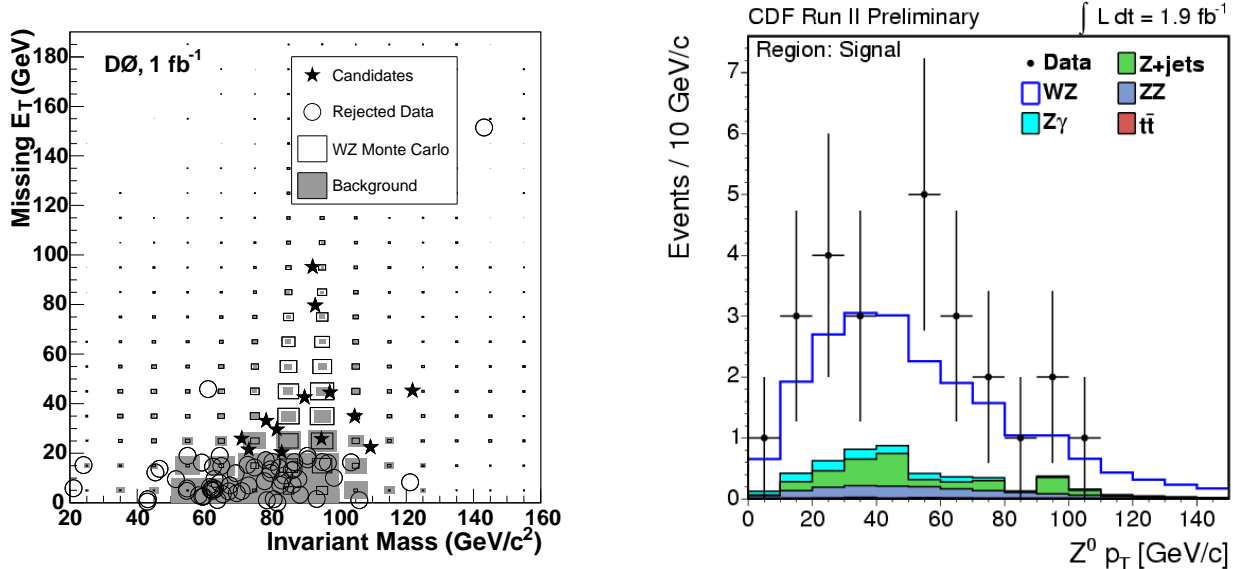


FIG. 2: Left: Missing  $E_T$  versus dilepton invariant mass for  $D\bar{O}$   $WZ \rightarrow \ell\ell\nu$  candidate events [10]. The open boxes represent the expected  $WZ$  signal. The gray boxes represent the sum of the estimated backgrounds. The black stars are the data that survive all selection criteria. The open circles are data that fail either the dilepton invariant mass criterion or have low missing  $E_T$ . Right: Distributions of  $Z p_T$  for CDF  $WZ \rightarrow \ell\ell\nu$  candidate events (points), for various expected background processes (hatched histograms) and for signal+background (open histograms) [14].

Non-SM couplings enhance  $WW$  production cross section, particularly at high values of the boson  $p_T$ . To probe  $WWZ/WW\gamma$  TGCs, observed  $p_T$  spectrum of the two leptons are fitted to the templates of the  $WW$  MC events produced for scanned values of the non-SM couplings. Figure 1 (left) shows distribution of the leading lepton  $p_T$  in  $WW \rightarrow e^\pm\mu^\mp$  candidate events together with the expected distributions from the SM, and for the two representative values of the non-SM couplings [8]. Figure 1 (right) shows one- and two-dimensional 95% C.L. limits on  $\Delta\kappa$  and  $\lambda$  parameters at  $\Lambda=2.0$  TeV. The limits are derived under the assumption of equal  $WWZ$  and  $WW\gamma$  couplings. Table I summarizes obtained limits on anomalous  $WWZ$  and  $WW\gamma$  couplings for various values of  $\Lambda$  parameter and for four different assumptions on anomalous coupling interrelations. In the first relationship, the  $WW\gamma$  and  $WWZ$  parameters are equal; the second relationship, the HISZ parametrization [9] imposes  $SU(2) \times U(1)$  symmetry upon the coupling parameters; for the two other relationships, either the SM  $WW\gamma$  or  $WWZ$  interaction is fixed, while the other parameters are allowed to vary. In all cases, parameters which are not constrained by the coupling relationships are set to their SM values.

### III. $WZ \rightarrow \ell\ell\nu$ PRODUCTION

$WZ$  production, when accompanied with leptonic decays of both bosons,  $W \rightarrow \ell\nu$ ,  $Z \rightarrow \ell\ell$ , gives very distinct experimental signature. The final states contain three high- $p_T$  isolated leptons, of which at least two have the same flavor and the invariant mass consistent with  $M_Z$ , and large missing  $E_T$  and transverse mass  $M_T(\ell, E_T^{miss})$ . Backgrounds arise from  $Z$ +jets,  $Z\gamma$ ,  $ZZ$  and  $t\bar{t}$  productions.

CDF and  $D\bar{O}$  Collaborations have both studied  $WZ$  production [10, 11, 12, 13, 14]. The signal has been established at more than  $5\sigma$  statistical level by CDF with  $1.1 \text{ fb}^{-1}$  of data [12]. Measured cross sections are  $\sigma(WZ) = 2.7_{-1.3}^{+1.7}$  pb by  $D\bar{O}$  with  $\mathcal{L} = 1.0 \text{ fb}^{-1}$  [10], and  $\sigma(WZ) = 4.3_{-1.0}^{+1.3}$  (stat)  $\pm 0.2$  (syst)  $\pm 0.3$  (lumi) pb by CDF with  $\mathcal{L} = 1.9 \text{ fb}^{-1}$  [13]. These agree with the SM NLO prediction of  $\sigma(WZ) = 3.68 \pm 0.25$  pb [5]. Figure 2 (left) shows distribution of  $E_T^{miss}$  versus dilepton invariant mass in  $D\bar{O}$   $WZ \rightarrow \ell\ell\nu$  candidate events together with the expected  $WZ$  signal and the estimated backgrounds.

TABLE II: One-dimensional 95 % C.L. limits obtained by  $D\mathcal{O}$  and CDF in  $WWZ$  analysis. The limits correspond to form factor scale of  $\Lambda = 2$  TeV.

$D\mathcal{O}, \mathcal{L} = 1.1 \text{ fb}^{-1}$ [10]	CDF, $\mathcal{L} = 1.9 \text{ fb}^{-1}$ [14]
$-0.17 < \lambda_Z < 0.21$	$-0.13 < \lambda_Z < 0.14$
$-0.14 < \Delta g_Z < 0.34$	$-0.13 < \Delta g_Z < 0.23$
$-0.12 < \Delta \kappa_Z = \Delta g_Z < 0.29$	$-0.76 < \Delta \kappa_Z = \Delta g_Z < 1.18$

The Fermilab Tevatron currently is the only particle accelerator that can produce the charged state  $WZ$ . The  $WZ$  events provide a unique opportunity to study the  $WWZ$  TGCs without any assumption on the values of the  $WW\gamma$  couplings. As discussed in the previous section, measurements of TGCs using the  $WW$  events are sensitive to both the  $WW\gamma$  and  $WWZ$  couplings at the same time and must make some assumption as to how they are related to each other. Non-SM anomalous TGCs will enhancement the  $WZ$  production cross section, and modify the shapes of kinematic distributions, such as the  $W$  and  $Z$  bosons transverse momenta. By comparing the measured cross section and  $P_T^Z$  distribution to the SM prediction and to models with anomalous TGCs, the Tevatron experiments set limits on the three coupling parameters:  $\lambda_Z$ ,  $\Delta g_1^Z$ , and  $\Delta \kappa_Z$ . A comparison of the observed  $Z$  boson  $p_T$  distribution in CDF data with SM predictions for signal and background is shown in Fig. 2 (right). The table II summarizes obtained 95% C.L. limits on the coupling parameters for the scale factor  $\Lambda = 2$  TeV.

#### IV. $WW/WZ \rightarrow \ell\nu jj$ PRODUCTION

The CDF Collaboration has also searched  $WW/WZ$  production in the  $\ell\nu jj$  final state [15]. The signature arises when  $W$  decays leptonically,  $W \rightarrow \ell\nu$ , and the associated boson decays hadronically,  $W/Z \rightarrow jj$ . The resulting final state is similar to that of Higgs production in  $WH \rightarrow \ell\nu b\bar{b}$  channel, and is experimentally much more challenging than the fully leptonic decay modes of  $WW$  and  $WZ$  productions. The background arises due to  $W/Z$ +jets, QCD multijet,  $t\bar{t}$  events. After selecting events with a high- $p_T$  lepton, large missing  $E_T$  and transverse mass  $M_T(\ell, E_T^{miss})$ , and  $\geq 2$  jets, signal/background ratio is less than 1%. Several discriminating kinematic variables are combined into Neural Net to achieve further separation of the signal from the background. Finally, the signal is extracted by fitting observed dijet mass  $M(jj)$  distribution to the templates of the expected signal and background distributions.

Figure 3 shows distribution of the dijet invariant mass in the candidate events after subtracting background

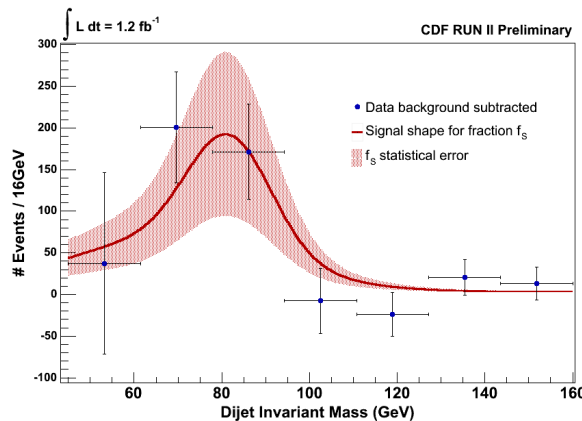


FIG. 3: Background subtracted distribution of dijet invariant mass in CDF  $WW/WZ \rightarrow \ell\nu jj$  candidate events [15].

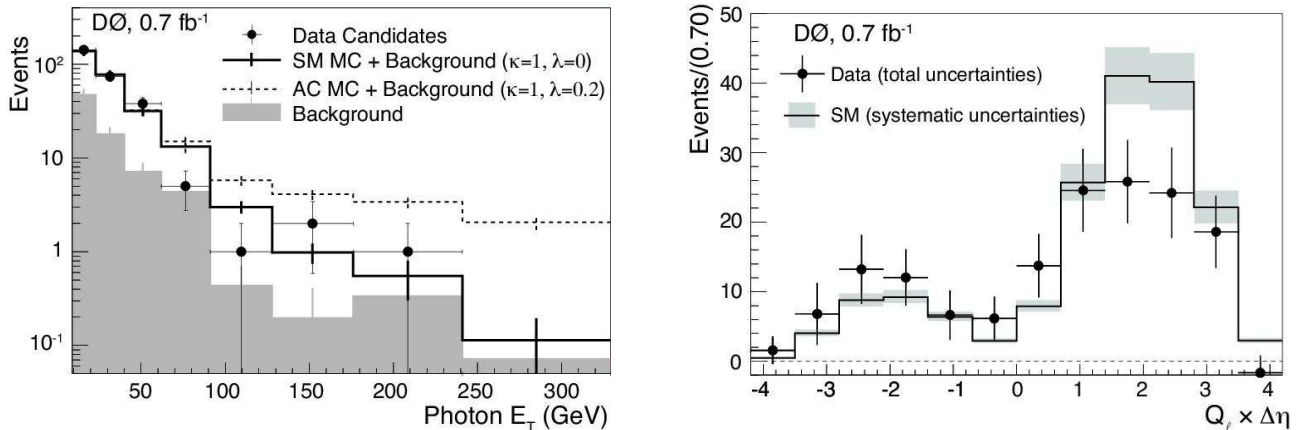


FIG. 4: Left: photon  $E_T$  distribution for  $D\bar{0}$   $W\gamma$  candidate events (points), and for the expected SM signal + background (open solid-line histogram). The shaded histogram shows background contribution. Dashed histogram corresponds to the non-SM coupling for  $WW\gamma$  [19]. Right: The background-subtracted charge-signed rapidity difference for the  $D\bar{0}$   $W\gamma$  candidate events (points), and for the expected SM signal + background (histogram) [19].

contribution. Measured cross section times branching ratio is  $\sigma \times BR = 1.47 \pm 0.77$  (stat) $\pm 0.38$  (syst) pb. Since observed signal has less than  $3\sigma$  statistical significance, 95 % C.L. limit is also set on the cross section times branching ratio:  $\sigma \times BR < 2.88$  pb. The results are in agreement with the theory calculations of  $\sigma \times BR = 2.09 \pm 0.14$  pb [5].

## V. $W\gamma \rightarrow \ell\nu\gamma$ PRODUCTION AND STUDY OF RADIATION AMPLITUDE ZERO

Production of  $W\gamma$  events at the Tevatron is studied in the leptonic decay mode of  $W \rightarrow \ell\nu$  which leads to the final state containing lepton, neutrino and a photon. The events are selected by requiring a high  $p_T$  lepton, large values of  $E_T^{miss}$  and transverse  $M_T(\ell, E_T^{miss})$ , and a photon with  $E_T$  above 7 or 8 GeV. The dominant background arises from  $W$ +jets production where a jet mimics a photon. Inclusive  $Z \rightarrow \ell\ell$  production and  $Z\gamma$  events can also contribute to the background. Both,  $D\bar{0}$  and CDF Collaborations have measured  $W\gamma$  production cross section [16, 17] and found good agreement with the SM expectation.

At leading order, the SM allows production of  $p\bar{p} \rightarrow q\bar{q}' \rightarrow W\gamma$  via photon radiation off an incoming quark (initial state radiation) or directly through  $WW\gamma$  vertex. These two production mechanisms involve three amplitudes where each alone violates unitarity, but together interfere to give finite cross section. This interference leads to radiation-amplitude zero (RAZ) in the angular distribution of the photon. The RAZ manifests itself as a dip in the charge-signed rapidity difference between the photon and the charged decay lepton from the  $W$  boson,  $Q_\ell \times \Delta\eta = Q_\ell(\eta_\gamma - \eta_\ell)$  [18].

Non-SM  $WW\gamma$  couplings will give rise to an increase in the  $W\gamma$  production cross section over the SM prediction, particularly for energetic photons. Anomalous TGCs can also make RAZ dip more shallow or disappear entirely. Figure 4 (left) shows distribution of the photon  $E_T$  in  $D\bar{0}$   $W\gamma$  candidates together with the expected SM signal and background distributions. Example of distribution for non-SM  $W\gamma$  signal is also shown. In order to set limits on anomalous TGCs,  $W\gamma$  signal events are generated at various values of TGCs. Observed photon  $E_T$  spectrum is then compared to the expected ones to determine the likelihood that they represent the data. Obtained one-dimensional 95% C.L. limits by  $D\bar{0}$  are  $-0.51 < \Delta\kappa_\gamma < 0.51$  and  $-0.12 < \lambda_\gamma < 0.13$  for  $\Lambda = 2$  TeV [19].

Figure 4 (right) shows distribution of the background-subtracted  $Q_\ell \times \Delta\eta$  for  $W\gamma$  candidates in the  $D\bar{0}$  data together with the SM expectation. The dip in the distribution at  $Q_\ell \times \Delta\eta \simeq -0.3$  is clearly visible. In order to evaluate the significance of the observation, a set of anomalous coupling which provides a  $Q_\ell \times \Delta\eta$  distribution

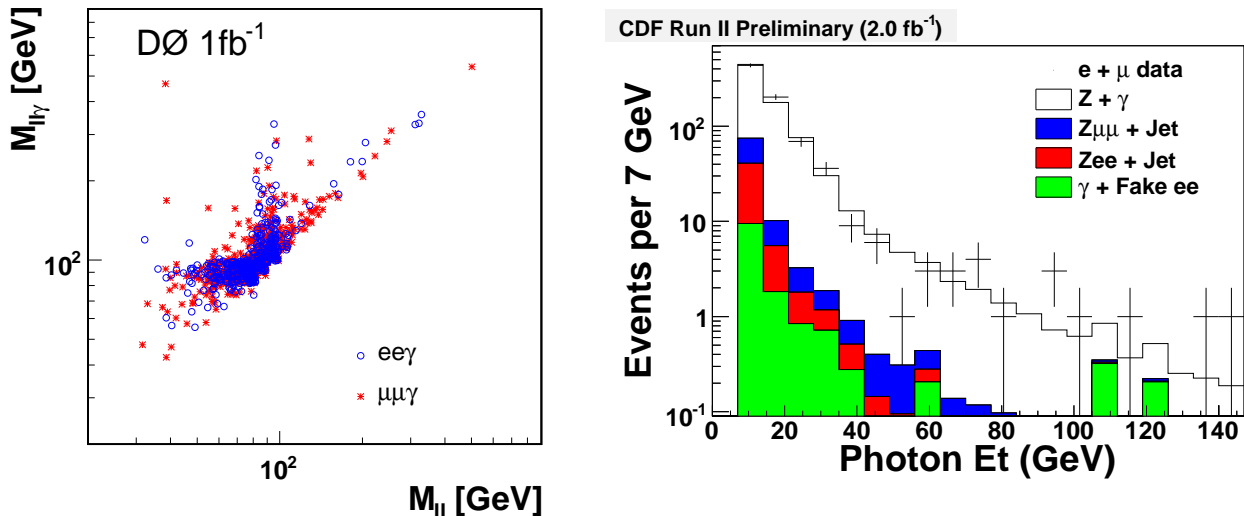


FIG. 5: Left: Dilepton + photon vs. dilepton mass in  $DØ Z\gamma \rightarrow ee\gamma/\mu\mu\gamma$  candidate events [20]. Masses of the candidates in electron channel are shown as open circles, while those in the muon channel are shown as stars. Right: Observed (points) and expected (histograms) distributions of photon  $E_T$  in CDF  $Z\gamma \rightarrow ee\gamma/\mu\mu\gamma$  analysis [22].

that minimally exhibits no dip is selected. This corresponds to  $\kappa_\gamma = 0$  and  $\lambda_\gamma = -1$  values of TGCs. For this set, probability to observed the dip due to the random fluctuation is estimated to be  $4.5 \times 10^{-3}$  corresponding to  $2.6 \sigma$  Gaussian significance. This constitutes the first indication of RAZ in  $W\gamma$  production [19].

## VI. $Z\gamma \rightarrow \ell\ell\gamma$ PRODUCTION

Production of  $p\bar{p} \rightarrow q\bar{q} \rightarrow Z\gamma$  events at the Tevatron is studied in  $Z\gamma \rightarrow \ell^+\ell^-\gamma$  channel. The signal sample is selected by requiring a pair of either muon or electron, and a photon. The photon can be produced by final state radiation (FSR) off either charged leptons or one of the initial partons (ISR). The main background process is  $Z + jet$  production where a jet is misidentified as a photon. Both Tevatron experiments have measured cross section times branching ratio for the  $p\bar{p} \rightarrow q\bar{q} \rightarrow Z\gamma$  production. Figure 5 (left) shows dilepton + photon vs. dilepton mass distribution for  $DØ Z\gamma \rightarrow ee(\mu\mu)\gamma$  candidate events. The observed structure reflects three sub-processes: the vertical band with  $M_{\ell\ell} \simeq M_Z$  and  $M_{\ell\ell\gamma} > M_Z$  corresponds to ISR production; the horizontal band at  $M_{\ell\ell\gamma} \simeq M_Z$  and  $M_{\ell\ell} < M_Z$  corresponds to FSR events; the Drell-Yan events populate the diagonal band with  $M_{\ell\ell} \simeq M_{\ell\ell\gamma}$ .

Using  $\mathcal{L} = 1 \text{ fb}^{-1}$  of data,  $DØ$  has obtained  $\sigma \times BR(Z\gamma \rightarrow \ell\ell\gamma) = 4.96 \pm 0.30 \text{ (stat+syst)} \pm 0.30 \text{ (lumi)}$  pb for  $M(\ell\ell) > 30 \text{ GeV}$ ,  $E_T^\gamma > 7 \text{ GeV}$  and  $dR(\ell\gamma) > 0.7$  [20]. The latter requirement minimizes contribution from the FSR sub-process. The measurement is in agreement with NLO SM expectation of  $\sigma \times BR(Z\gamma \rightarrow \ell\gamma) = 4.74 \pm 0.22 \text{ pb}$  [21]. CDF has measured  $\sigma \times BR(Z\gamma \rightarrow \ell\ell\gamma)$  separately for ISR enriched ( $M(\ell\ell\gamma) > 100 \text{ GeV}$ ) and FSR enriched ( $M(\ell\ell\gamma) < 100 \text{ GeV}$ ) productions obtaining  $\sigma \times BR(Z\gamma \rightarrow \ell\ell\gamma) = 1.2 \pm 0.1 \text{ (stat)} \pm 0.2 \text{ (syst)} \pm 0.1 \text{ (lumi)}$  pb, and  $\sigma \times BR(Z\gamma \rightarrow \ell\ell\gamma) = 3.4 \pm 0.2 \text{ (stat)} \pm 0.2 \text{ (syst)} \pm 0.2 \text{ (lumi)}$  pb, respectively [22]. The measurements use  $\mathcal{L} = 1.1(2.0) \text{ fb}^{-1}$  of data for  $Z\gamma \rightarrow ee\gamma (\mu\mu\gamma)$  channel and are in good agreement with the SM NLO theory calculations.

Most general effective Lagrangian that assumes Lorentz and gauge invariance, has two CP-violating ( $h_1^V$  and  $h_2^V$ ) and two CP-conserving ( $h_3^V$  and  $h_4^V$ ) parameters for anomalous trilinear  $ZV\gamma$  ( $V = Z, \gamma$ ) couplings. Unitarity is ensured by using form factor parametrization  $h_i^V = \frac{h_{i0}^V}{(1+\hat{s}/\Lambda^2)^n}$ , with  $\Lambda$  being a form factor scale,  $h_{i0}^V$  being the low-energy approximations of the couplings, and  $n=3(4)$  for  $h_{1,3}^V(h_{2,4}^V)$  [23]. Parameters  $h_i^V$  are all zero in the SM. Non-zero  $h_i^V$  couplings typically enhance  $Z\gamma$  production cross section, particularly at high

TABLE III: One-dimensional 95 % C.L. limits on anomalous neutral TGCs obtained by DØ and CDF in  $Z\gamma$  analysis. The limits correspond to form factor scale  $\Lambda = 1.2$  TeV.

DØ, $\mathcal{L} = 1 \text{ fb}^{-1}$ [20]	CDF, $\mathcal{L} = 1.1\text{-}2.0 \text{ fb}^{-1}$ [22]
$-0.085 < h_3^\gamma < 0.084$	$-0.084 < h_3^\gamma < 0.084$
$-0.0053 < h_4^\gamma < 0.0054$	$-0.0047 < h_4^\gamma < 0.0047$
$-0.083 < h_3^Z < 0.082$	$-0.083 < h_3^Z < 0.083$
$-0.0053 < h_4^Z < 0.0054$	$-0.0047 < h_4^Z < 0.0047$

values of photon  $E_T$ . The  $E_T$  distribution of the photon for CDF  $Z\gamma$  candidate events, compared with the background and the SM  $Z\gamma$  prediction is shown in Fig. 5 (right). To set limits on anomalous  $ZZ\gamma$  and  $Z\gamma\gamma$  couplings, photon  $E_T$  distribution in data is compared with the expected  $E_T$  distribution from anomalous  $Z\gamma$  production for a given set of  $ZZ\gamma$  and  $Z\gamma\gamma$  coupling values. Limits on anomalous TGCs obtained by DØ and CDF Collaborations are summarized in Table III. Obtained limits on  $h_{40}^V$  are the most stringent to date.

## VII. $ZZ \rightarrow llll$ AND $ZZ \rightarrow ll\nu\nu$ PRODUCTIONS

The NLO SM cross section for  $p\bar{p} \rightarrow ZZ$  production at  $\sqrt{s} = 1.96$  TeV is  $\sigma(ZZ) = 1.4 \pm 0.1$  pb [24]. The process has been studied in two decay modes at the Tevatron:  $ZZ \rightarrow llll$  and  $ZZ \rightarrow ll\nu\nu$  channels. The first mode is experimentally very clean giving rise to events with four high- $p_T$  isolated leptons and very little hadronic activity. However, it also suffers from low branching fraction of  $4.5 \times 10^{-3}$ , with total expected number of  $ZZ \rightarrow llll$  events being 6.3 per  $\text{fb}^{-1}$ . This is further reduced by kinematic selection and lepton identification requirements. Background to  $ZZ \rightarrow llll$  signal arises from  $Z(\gamma) + jets$  and  $t\bar{t}$  production processes and is typically orders of magnitude smaller compared to the signal.  $ZZ \rightarrow ll\nu\nu$  channel has higher branching fraction, but also higher background contamination mainly from  $WW$ ,  $Z + jets$  and  $WZ$  productions which can all produce events with two high- $p_T$  lepton and missing  $E_T$ .

DØ and CDF experiments have both studied  $ZZ$  production in  $ZZ \rightarrow llll$  and  $ZZ \rightarrow ll\nu\nu$  channels. In  $\mathcal{L} = 1.9 \text{ fb}^{-1}$  of data, CDF has observed 3  $ZZ \rightarrow llll$  candidates with expected background of  $0.096_{-0.063}^{+0.092}$  events. Figure 6 (left) shows four-lepton invariant mass distribution for the three observed events, as well as expected distributions for the background and the signal. For  $ZZ \rightarrow ll\nu\nu$  channel, a leading order calculations of the relative  $ZZ$  and  $WW$  event probabilities is used to discriminate between signal and background. Combination of  $ZZ \rightarrow llll$  and  $ZZ \rightarrow ll\nu\nu$  channels leads to observation of excess over expected background at the level of  $4.4 \sigma$  statistical significance. The measured combined cross section of  $\sigma(p\bar{p} \rightarrow ZZ) = 1.4_{-0.6}^{+0.7}$  (stat+syst) pb [25] is consistent with the NLO SM expectation [24].

In  $\mathcal{L} = 1 \text{ fb}^{-1}$  of data DØ has observed one  $ZZ \rightarrow llll$  candidate with expected signal and background rates being  $1.71 \pm 0.15$  and  $0.13 \pm 0.03$  events, respectively. This gives 95% C.L. upper limit of 4.4 pb for  $ZZ$  production cross section [26]. For  $ZZ \rightarrow ll\nu\nu$  channel, several kinematic variables have been combined in likelihood discriminant to achieve good signal-to-background discrimination. Figure 6 (right) shows likelihood distribution for data and for expected signal and background in  $ZZ \rightarrow \mu\mu\nu\nu$  channel. Obtained cross section value of  $\sigma(p\bar{p} \rightarrow ZZ) = 2.1 \pm 2.1$  (stat)  $\pm 0.4$  (syst) pb [27] is consistent with the NLO SM expectation [24].

Most general effective Lagrangian that assumes Lorentz and gauge invariance, has two CP-violating ( $f_4^V$ ) and two CP-conserving ( $f_5^V$ ) parameters for anomalous trilinear  $ZZV$  ( $V = Z, \gamma$ ) couplings. Unitarity is ensured by using form factor parametrization  $f_i^V = \frac{f_{i0}^V}{(1+\hat{s}/\Lambda^2)^3}$ , with  $\Lambda$  being a form factor scale and  $f_{i0}^V$  being the low-energy approximations of the couplings [28].  $ZZZ$  and  $ZZ\gamma$  vertices are all forbidden in the SM at the tree level. Non-SM couplings typically increase  $ZZ$  production cross section. Using observed and expected number of events for various assumptions on  $ZZZ$  and  $ZZ\gamma$  coupling values, DØ has derived limits on anomalous TGCs [26].

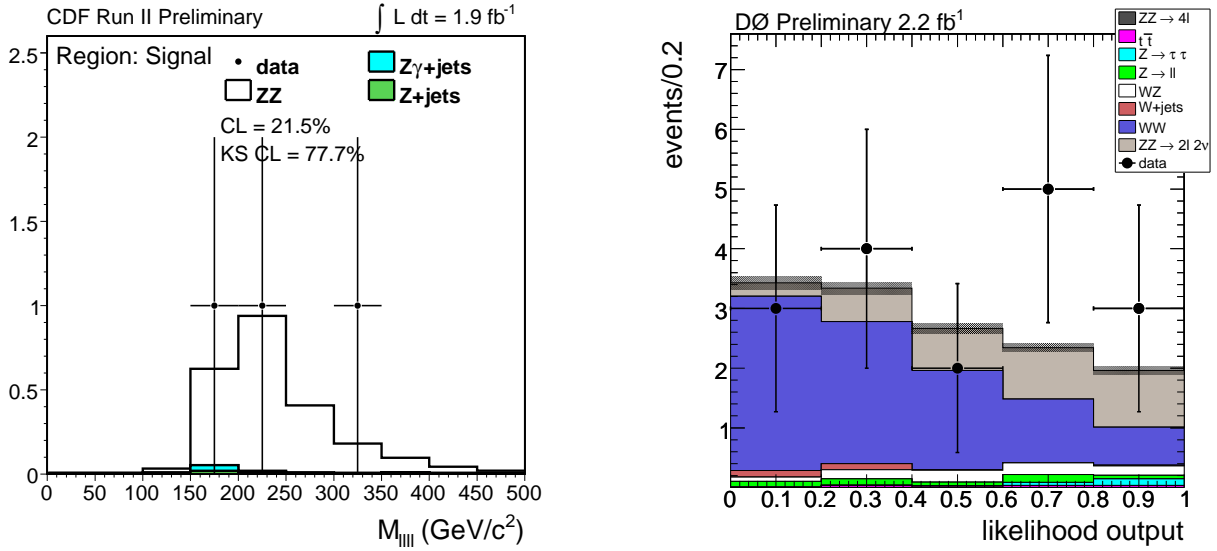


FIG. 6: Left: Observed (points) and expected distributions (histograms) of four lepton invariant mass in  $ZZ \rightarrow \ell\ell\ell\ell$  channel in CDF [25]. Right: Observed (points) and expected distributions (histograms) of event likelihood discriminant in  $ZZ \rightarrow \ell\nu\nu$  channel in DØ [27].

One-dimensional 95% C.L. limits are  $-0.28 < f_{40}^Z < 0.28$ ,  $-0.26 < f_{40}^\gamma < 0.26$ ,  $-0.31 < f_{50}^Z < 0.29$ ,  $-0.30 < f_{50}^\gamma < 0.28$ . The limits are competitive to those of the combined LEP experiments [29].

## VIII. SUMMARY

Productions of  $WW$ ,  $WZ$ ,  $W\gamma$ ,  $Z\gamma$ , and  $ZZ$  have all been studied at the Tevatron. Measured production cross sections for these processes are in agreement with the SM expectations. The diboson productions allow to directly probe Triple Gauge boson Couplings via observed event rates and kinematics. With no indication for the deviation from the SM expectation, limits are set on anomalous TGCs. First indication of the peculiar feature, such as Radiation Amplitude Zero, predicted by SM for the  $W\gamma$  production has also been observed.

## Acknowledgments

The author wishes to thank HCP2008 organizers for lively and constructive atmosphere at the conference.

- 
- [1] V.M. Abazov et al. (DØ Collaboration), “Measurement of the  $WW$  Production Cross Section in  $p\bar{p}$  collisions at  $\sqrt{s}=1.96$  TeV”, Phys. Rev. Lett. 94, 151801 (2005).
  - [2] D. Acosta et al., (CDF Collaboration), “Measurement of the  $W^+W^-$  Production Cross Section in  $p\bar{p}$  Collisions at  $\sqrt{s} = 1.96$  TeV using Dilepton Events”, Phys. Rev. Lett. 94, 211801 (2005).
  - [3] CDF Collaboration, “Measurement of the  $W^+W^-$  Production Cross Section in  $825 \text{ pb}^{-1}$  of  $p\bar{p}$  Collisions at  $\sqrt{s} = 1.96$  TeV using Dilepton Events”, <http://www-cdf.fnal.gov/physics/ewk/2006/ww/>
  - [4] J. Ohnemus, Phys. Rev. D 50, 1931 (1994).
  - [5] J.M. Campbell and R.K. Ellis, Phys. Rev. D 60, 113006 (1999).
  - [6] K. Hagiwara, R.D. Peccei, D. Zeppenfeld and K. Hikasa, Nucl. Phys. B 282, 253 (1987).
  - [7] U. Baur and D. Zeppenfeld, Nucl. Phys. B 308, 127 (1988).

- [8] V.M. Abazov et al. (DØ Collaboration), “Limits on anomalous trilinear gauge couplings from  $WW \rightarrow e^+e^-$ ,  $WW \rightarrow e^\pm\mu^\mp$ , and  $WW \rightarrow \mu^+\mu^-$  events from  $p\bar{p}$  collisions at  $\sqrt{s} = 1.96$  TeV”, Phys. Rev. D 74, 057101 (2006).
- [9] K. Hagiwara, S. Ishihara, R. Szalapski, and D. Zeppenfeld, Phys. Rev. D 48, 2182 (1993); the coupling relationships used are  $\Delta\kappa_Z = \Delta\kappa_\gamma(1 - \tan^2\theta_W)$ ,  $\Delta g_1^Z = \Delta\kappa_\gamma/(2\cos^2\theta_W)$  and  $\lambda_Z = \lambda_\gamma$ .
- [10] V.M. Abazov et al. (DØ Collaboration), “Measurement of the  $p\bar{p} \rightarrow WZ + X$  cross section at  $\sqrt{s} = 1.96$  TeV and limits on  $WWZ$  trilinear gauge couplings”, Phys. Rev. D 76, 111104 (R) (2007).
- [11] V.M. Abazov et al. (DØ Collaboration), “Production of  $WZ$  Events in  $p\bar{p}$  Collisions at  $\sqrt{s} = 1.96$  TeV and Limits on  $WWZ$  Couplings”, Phys. Rev. Lett. 95, 141802 (2005).
- [12] A. Abulencia et al. (CDF Collaboration), “Observation of  $WZ$  Production”, Phys. Rev. Lett. 98, 161801 (2007).
- [13] CDF Collaboration, “Measurement of  $WZ$  Production in  $WZ \rightarrow ll\nu$  using  $2 \text{ fb}^{-1}$  of  $p\bar{p}$  Collisions at  $\sqrt{s} = 1.96$  TeV”, [http://fcdwww.fnal.gov/physics/ewk/2007/WZ\\_2fb/](http://fcdwww.fnal.gov/physics/ewk/2007/WZ_2fb/)
- [14] CDF Collaboration, “ $WZ$  Anomalous Triple Gauge Couplings in  $1.9 \text{ fb}^{-1}$  of  $p\bar{p}$  Collisions at  $\sqrt{s} = 1.96$  TeV”, <http://fcdwww.fnal.gov/physics/ewk/2008/WZatgc/>
- [15] T. Aaltonen et al. (CDF Collaboration), “Search for  $WW/WZ \rightarrow \ell\nu jj$  at CDF using  $1.2 \text{ fb}^{-1}$  of data”, <http://www-cdf.fnal.gov/physics/ewk/2008/wwwz/>
- [16] V.M. Abazov et al. (DØ Collaboration), “Measurement of the  $p\bar{p} \rightarrow W\gamma + X$  cross section at  $\sqrt{s} = 1.96$  TeV and  $WW\gamma$  anomalous coupling limits”, Phys. Rev. D 71, 091108 (R) (2005).
- [17] CDF Collaboration, “Measurement of  $W\gamma$  Production in  $p\bar{p}$  Collisions at  $\sqrt{s} = 1.96$  TeV”, <http://fcdwww.fnal.gov/physics/ewk/2007/wgzg/>
- [18] U. Baur, S. Errede, and G. Landsberg, Phys. Rev. D 50, 1917 (1994).
- [19] V.M. Abazov et al. (DØ Collaboration), “First Study of the Radiation-Amplitude Zero in  $W\gamma$  Production and Limits on Anomalous  $WW\gamma$  Couplings at  $\sqrt{s} = 1.96$  TeV”, Phys. Rev. Lett. 100, 241805 (2008).
- [20] V.M. Abazov et al. (DØ Collaboration), “ $Z\gamma$  production and limits on anomalous  $ZZ\gamma$  and  $Z\gamma\gamma$  couplings in  $p\bar{p}$  collisions at  $\sqrt{s} = 1.96$  TeV”, Phys. Lett. B 653, 378 (2007).
- [21] U. Baur, T. Han, and J. Ohnemus, Phys. Rev. D 57, 2823 (1998).
- [22] T. Aaltonen et al. (CDF Collaboration), “ $Z\gamma$  Production and limits on Neutral Anomalous Coupling in  $p\bar{p}$  Collisions at  $\sqrt{s} = 1.96$  TeV and Limits on Neutral Anomalous Coupling”, <http://fcdwww.fnal.gov/physics/ewk/2008/Zgamma>
- [23] U. Baur and E. Berger, Phys. Rev. D 47, 4889 (1993).
- [24] J.M. Campbell and R.K. Ellis, Phys. Rev. D 60, 113006 (1999).
- [25] T. Aaltonen et al. (CDF Collaboration), “Strong Evidence for  $ZZ$  Production in  $p\bar{p}$  Collisions at  $\sqrt{s} = 1.96$  TeV”, Phys. Rev. Lett. 100, 201801 (2008).
- [26] V.M. Abazov et al. (DØ Collaboration), “Search for  $ZZ$  and  $Z\gamma^*$  Production in  $p\bar{p}$  Collisions at  $\sqrt{s} = 1.96$  TeV and Limits on Anomalous  $ZZZ$  and  $ZZ\gamma^*$  Couplings”, Phys. Rev. Lett. 100, 131801 (2008).
- [27] V.M. Abazov et al. (DØ Collaboration), “ $ZZ \rightarrow \ell^+\ell^-$  production in  $p\bar{p}$  collisions at  $\sqrt{s} = 1.96$  TeV”, DØ Note 5620-CONF, <http://www-d0.fnal.gov/Run2Physics/WWW/results/prelim/EW/E24/E24.pdf>
- [28] U. Baur and D. Rainwater, Phys. Rev. D 62, 113011 (2000).
- [29] The LEP Collaborations: ALEPH, DELPHI, L3, and OPAL, “A Combination of Preliminary Electroweak Measurements and Constraints on the Standard Model”, arXiv:hep-ex/0612034.